Tombari, A., Espinosa, G., Alexander, N., & Cacciola, P. (2018). Vibration control of a cluster of buildings through the Vibrating Barrier. *Mechanical Systems and Signal Processing*, *101*, 219-236. https://doi.org/10.1016/j.ymssp.2017.08.034

VIBRATION CONTROL OF A CLUSTER OF BUILDINGS THROUGH THE VIBRATING BARRIER

A. Tombari (1), M. Garcia Espinosa (2), N.A. Alexander (3), P. Cacciola (4)

(1) *University of Brighton, a.tombari@brighton.ac.uk*
(2) *University of Oxford, maria.garciaespinosa@linacre.ox.ac.uk*
(3) *University of Bristol, Nick.Alexander@bristol.ac.uk*
(4) *University of Brighton, p.cacciola@brighton.ac.uk*

Abstract

A novel device, called vibrating barrier (ViBa), that aims to reduce the vibrations of adjacent structures subjected to ground motion waves has been recently proposed. The ViBa is a structure buried in the soil and detached from surrounding buildings that is able to absorb a significant portion of the dynamic energy arising from the ground motion. The working principle exploits the dynamic interaction among vibrating structures due to the propagation of waves through the soil, namely the structure–soil–structure interaction. In this paper the efficiency of the ViBa is investigated to control the vibrations of a cluster of buildings. To this aim, a discrete model of structures-site interaction involving multiple buildings and the ViBa is developed where the effects of the soil on the structures, i.e. the soil-structure interaction (SSI), the structure-soil-structure interaction (SSSI) as well as the ViBa-soil-structures interaction are taken into account by means of linear elastic springs. Closed-form solutions are derived to design the ViBa in the case of harmonic excitation from the analysis of the discrete model. Advanced finite element numerical simulations are performed in order to assess the efficiency of the ViBa for protecting more than a single building. Parametric studies are also conducted to identify beneficial/adverse effects in the use of the proposed vibration control strategy to protect cluster of buildings. Finally, experimental shake table tests are performed to a prototype of a cluster of two buildings protected by the ViBa device for validating the proposed numerical models.

Keywords: Vibrating Barrier; ViBa; structure-soil-structure interaction; cluster of buildings; shake table testing; seismic vibration control.

1. Introduction

Recent earthquake events such as L'Aquila in Italy, 2009, Port-au-Prince in Haiti, 2010, Lamjung in Nepal, 2015, and Amatrice in Italy, 2016, pointed out the problematic of protecting wide urban areas in which historical buildings are hosted.

Whilst seismic protection of new buildings is commonly addressed through a proper seismic design of the structure or by using devices such as isolators, dampers as well as tuned mass dampers, the rehabilitation of existing buildings is a complex task that generally requires impacting structural interventions that, in case of heritage buildings, can alter their architectural value. Furthermore, similar expensive interventions are rarely employed for private constructions letting a huge number of towns and cities worldwide below the adequate level of seismic safety. This situation is extremely concerning because in addition to the need of conservation of the architectural value and the relevant economic impact still a large death toll are occurring after a strong earthquake event.

Therefore, as traditional localised solutions might become impractical or difficult to apply to existing buildings alternative solutions need to be pursued. One possible strategy is to protect the structures through trenches or sheet-pile walls in the soil (see e.g. Woods, [1]) for altering the displacement field based on the reflection, scattering and diffraction of dynamic surface waves or through the use of most innovative solutions, such as the resonant metawedge (Colombi et al., [2]) and other engineering metamaterials (see e.g. [3-7]) for controlling the flow of Rayleigh waves. However, this approach is more effective for surface waves rather than body waves. Cacciola and Tombari [8] introduced for the first time, a non-localized solution, called Vibrating Barrier (ViBa), hosted in the soil and detached from the structures, that exploits the structure-soil-structure mechanism for reducing the vibrations of structures due to ground motion excitation. Analyses on the efficiency of the ViBa in

protecting a single building are reported in Cacciola and Tombari [8], in Cacciola et al. [9] for structure founded on monopile foundation and in Tombari et al. [10] for an industrial building.

Furthermore, as non-local solution, the Vibrating Barrier can be used to mitigate more than one building making it suitable for its installation in the urban environment.

The seismic free-field wavefield is greatly affected by the collective behaviour of the buildings especially in densely populated urban environment; this effect is referred to as “city effect” or “site-city Interaction”, and several studies have been undertaken in the last decades in this regard, see e.g. Clouteau and Aubry [11], Chávez-García and Cárdenas [12], Guéguen et al. [13], Kham et al. [14], Ghergu and Ionescu [15], Isbiliroglu et al. [16], Schwan et al. [17] and Guéguen and Colombi [18], just to cite a few. In particular, Kham et al. [14] showed that the energy of ground motion in a city can be reduced or increased due to the perturbation induced by resonant buildings. This phenomenon, that globally governs the site–city effects, can be seen as an extension of the structure–soil–structure interaction (SSSI).

In particular, the first studies on SSSI were carried out by Warburton et al. [19] on the dynamic response of two rigid masses in an elastic subspace, where they highlighted the influence of one mass on the dynamic response of the other. The dynamic interaction between two parallel infinite shear walls placed on rigid foundations and forced by a vertically incident shear (SH) wave was investigated by Luco & Contesse [20]. Wong & Trifunac [21] extended the previous case for non-vertically incident plane SH waves by investigating the significance of the angle of incidence. A comprehensive review of the SSSI problem can be found in Lou et al. [22].

In this framework, the Vibrating Barrier interacts with the adjacent structures and mitigates their vibrations if opportunely designed. It is noted that this approach differs substantially from the recent proposed seismic metamaterials (see e.g. [2-7]), which aim to deviate the surface seismic waves away from the structure, while the Vibrating Barrier is conceived to

absorb the seismic body waves. Also, it has to be emphasized that the ViBa, as a difference from the metamaterials, exploits the structure-soil-structure interaction phenomenon that modifies the dynamic properties of the neighbouring structures. The tuning of the ViBa is addressed via a discrete model, following the approach proposed in literature for discrete SSSI problems. Specifically, Kobori et al. [23] defined a multi-spring–mass system for investigating the dynamic coupling of two adjacent square superficial foundations. Mulliken and Karabalis [24] defined a simple discrete model for predicting the dynamic interaction between adjacent rigid surface foundations supported by a homogeneous, isotropic and linear elastic half-space. Recently, Alexander et al. [25] developed a discrete model to study the SSSI problem of surface foundations by considering stochastic ground motion excitation which has been extended by Aldaikh et al. [26-27] to the case of three buildings and validated by means of experimentally shake-table testing.

In this paper, a discrete model comprised of masses and linear visco-elastic springs is used for simulating the soil-structure interaction (SSI), the structure-soil-structure interaction (SSSI) as well as the ViBa-soil-structure interaction. An analytical formula for tuning the ViBa in the case of two adjacent buildings, is determined. A parametric investigation is also performed to highlight the efficiency of the ViBa. A prototype comprised of two structures and the ViBa is realized and pertinent experimental tests have been also conducted. Specifically, the soil is represented by silicone rubber material, following the approach of Niwa et al. [28] and Kitada et al. [29] for the study of the SSSI for nuclear power plants. Furthermore, finite element analyses, validated through the experimental results, have been determined for evaluating the influence of the position of the ViBa on the dynamic response of the structures. The main aim of this paper is to demonstrate the efficiency of the Vibrating Barrier (originally proposed by Cacciola and Tombari [8]) for a cluster of buildings under harmonic excitations, through extensive parametric, numerical and experimental approaches.

2. General formulation of the governing equations

The problem analysed in this paper deals with the design of the Vibrating Barrier (ViBa) in order to reduce the vibration of the surrounding buildings as depicted in Fig. 1a. The vibration control of a cluster of buildings is carried out by deriving the dynamic governing equations in finite element formulation as illustrated in Fig. 1b; therefore, in this section, a general matrix formulation of the global problem is addressed. The mathematical expression, derived in terms of absolute displacements as it is conventional in soil-structure interaction, is stated as:

$$\left(\widetilde{\mathbf{K}} - \omega^2 \mathbf{M}\right)\mathbf{U}(\omega) = \mathbf{Q}\,\mathrm{U_g}(\omega) \qquad (1)$$

where $\mathbf{M}$ is the global mass matrix and $\widetilde{\mathbf{K}}$ is the complex stiffness matrix. The complex formulation of the stiffness, $\widetilde{\mathbf{K}}$, is obtained by populating each component of the matrix with the hysteretic damping model (see e.g. Kramer, [30]) , $\tilde{k} = k(1 + \mathrm{i}\eta)$, in which $\mathrm{i} = \sqrt{-1}$ and η is the material loss factor, the symbol $\widetilde{\square}$ indicates the complex stiffness quantities. It is worth mentioning that the complex formulation can be used to achieve the viscous damping model whereas the loss factor η is replaced with the viscous coefficient, c, by adopting the following expression $c = \frac{k\eta}{\omega}$, where ω is the circular frequency.

The absolute displacement vector $\mathbf{U}(\omega)$, formulated the frequency domain, lists the degrees of freedom (DOFs) of the whole global system, comprised of the soil, the buildings and the ViBa. The buildings and the soil are described by consistent matrices obtained by resorting to a traditional finite element method. The ViBa is described by a matrix $\widetilde{\mathbf{K}}_{\mathrm{V}}$ that includes the internal oscillating system and its box-foundation.

According to the displacement vector $\mathbf{U}(\omega)$, the matrices of the global system can be partitioned in the sub-matrices defined for the individual buildings and the ViBa; the global stiffness matrix $\widetilde{\mathbf{K}}$ is a block-matrix partitioned in the following form:

$$\widetilde{\mathbf{K}} = \begin{bmatrix} \widetilde{\mathbf{K}}_{1} & \widetilde{\mathbf{K}}_{1,\mathrm{i}} & \cdots & \widetilde{\mathbf{K}}_{1,n} & \widetilde{\mathbf{K}}_{1,\mathrm{V}} \\ \mathbf{K}_{\mathrm{i},1} & \widetilde{\mathbf{K}}_{\mathrm{i}} & & \widetilde{\mathbf{K}}_{\mathrm{i},n} & \widetilde{\mathbf{K}}_{\mathrm{i,V}} \\ \vdots & & \ddots & & \vdots \\ \widetilde{\mathbf{K}}_{n,1} & \widetilde{\mathbf{K}}_{n,\mathrm{i}} & \cdots & \widetilde{\mathbf{K}}_{n} & \widetilde{\mathbf{K}}_{n,\mathrm{V}} \\ \widetilde{\mathbf{K}}_{\mathrm{V},1} & \widetilde{\mathbf{K}}_{\mathrm{V,i}} & & \widetilde{\mathbf{K}}_{\mathrm{V,n}} & \widetilde{\mathbf{K}}_{\mathrm{V}} \end{bmatrix} \tag{2}$$

The main diagonal sub-matrices $\widetilde{\mathbf{K}}_{\mathrm{r}}$ (r = 1, … , n) describe the stiffness matrix of the rth-structure and its interaction with the soil. Lastly, the off-diagonal sub-matrices $\widetilde{\mathbf{K}}_{\mathrm{i,j}}$ ($i, j = 1, \dots, n; V$) are related to the dynamic coupling between structures and between the structures and ViBa.

On the other hand, the global mass matrix is a block-diagonal matrix stated as follows:

$$\mathbf{M} = \begin{bmatrix} \mathbf{M}_{1} & \mathbf{0} & \cdots & \mathbf{0} & \mathbf{0} \\ \mathbf{0} & \mathbf{M}_{\mathrm{i}} & & \mathbf{0} & \mathbf{0} \\ \vdots & & \ddots & \vdots & \\ \mathbf{0} & \mathbf{0} & & \mathbf{M}_{n} & \mathbf{0} \\ \mathbf{0} & \mathbf{0} & \cdots & \mathbf{0} & \mathbf{M}_{\mathrm{V}} \end{bmatrix} \tag{3}$$

in which $\mathbf{M}_{\mathrm{r}}$, for r = 1, … , n, in the jth sub-block is the consistent mass matrix of the jth building, while $\mathbf{M}_{\mathrm{V}}$ is the block-diagonal mass matrix of the ViBa given by

$$\mathbf{M}_{\mathrm{V}} = \begin{bmatrix} \mathbf{M}_{\mathrm{ViBa}} & 0 \\ 0 & \mathbf{M}_{\mathrm{f,ViBa}} \end{bmatrix} \tag{4}$$

defined by the mass matrix of the ViBa, $\mathbf{M}_{\mathrm{ViBa}}$, and by the mass matrix of its foundation, $\mathbf{M}_{\mathrm{f,ViBa}}$.

Finally, in Eq. (1), $\mathrm{U}_{\mathrm{g}}(\omega)$ is the Fourier transform of the ground displacement $u_{\mathrm{g}}(t)$, while the vector $\mathbf{Q}$ is the soil influence vector depending by the soil-foundation complex stiffness values obtained as $\mathbf{Q} = \widetilde{\mathbf{K}}\,\boldsymbol{\tau}$ where $\boldsymbol{\tau}$ is the unitary vector with ones at the structural foundation degree of freedom and having zeros elsewhere. It is worth mentioning that by introducing properly the influence matrix $\mathbf{Q}$, ground spatial variation of the input motion can be also considered due to the formulation of Eq. (1) in absolute displacements. However, it is noted that the use of absolute displacements needs particular attention as databases

general have erroneous ground motion displacement time series (see Chanerley and Alexander [31]).

3. Design of the Vibrating Barrier

The Vibrating barrier aims to reduce the vibrations of the adjacent structures and the consequent stresses related to the relative displacements. Therefore, the optimization problem is set as:

$$\begin{gathered} \min\left\{u_{\mathrm{i}}^{\mathrm{r,max}}(\mathrm{t},\boldsymbol{\alpha})\right\} \text{ for } \mathrm{i}=1,\ldots,n \\ \boldsymbol{\alpha}=\left\{\mathrm{k}_{\mathrm{ij}}^{\mathrm{V}},\eta_{\mathrm{ij}}^{\mathrm{V}},\mathrm{m}_{\mathrm{ii}}^{\mathrm{V}}\right\}\in\mathbb{R}_0^+ \text{ for } \mathrm{i},\mathrm{j}=1,\ldots,m \end{gathered} \tag{5}$$

Where $\mathbb{R}_0^+$ means the domain of strictly positive real numbers, $\mathrm{k}_{\mathrm{ij}}^{\mathrm{V}}$ and $\eta_{\mathrm{ij}}^{\mathrm{V}}$ are the stiffness and damping components of the $m \times m$ matrix $\widetilde{\mathbf{K}}_{\mathrm{V}}$; $\mathrm{m}_{\mathrm{ii}}^{\mathrm{V}}$ is the mass component of $\mathbf{M}_{\mathrm{V}}$; finally, $u_{\mathrm{i}}^{\mathrm{r,max}}(\mathrm{t},\boldsymbol{\alpha})$ is the maximum displacement of the ith structure relative to its foundation:

$$u_{\mathrm{i}}^{\mathrm{r,max}}(\mathrm{t},\boldsymbol{\alpha})=\max(u(\mathrm{t},\boldsymbol{\alpha})-u_{f,\mathrm{i}}(\mathrm{t},\boldsymbol{\alpha})) \tag{6}$$

and $\boldsymbol{\alpha}$ is the vector listing the design parameters. The time formulation of the displacements of Eq. (6) is obtained by inverse Fourier transformation of the displacements obtained from Eq. (1).

In case of harmonic input, the optimization procedure of Eq. (5) is rewritten in terms of transfer functions. By defining the dynamic stiffness matrix as

$$\widetilde{\mathbf{K}}_{\mathrm{dyn}}(\boldsymbol{\alpha},\omega)=\widetilde{\mathbf{K}}(\boldsymbol{\alpha})-\omega^2\mathbf{M}(\boldsymbol{\alpha}), \tag{7}$$

the governing equation of the motion Eq. (1) can be rewritten as follows:

$$\widetilde{\mathbf{K}}_{\mathrm{dyn}}(\boldsymbol{\alpha},\omega)\mathbf{U}(\omega)=\mathbf{Q}\,\mathrm{U}_{\mathrm{g}}(\omega) \tag{8}$$

Therefore, the dimensionless transfer function vector $\mathbf{H}(\boldsymbol{\alpha},\omega)$ is derived as follows:

$$\mathbf{H}(\boldsymbol{\alpha}, \omega) = \widetilde{\mathbf{K}}_{\mathrm{dyn}}^{-1}\mathbf{Q} \tag{9}$$

It is worth to emphasize that various objective functions of the optimization problem of Eq. (5) can be selected (e.g. see Cacciola et al. [9]). Clearly the optimization procedure will lead to different design parameters that better suit to different objectives. The main aim of this paper is to show the ability of the proposed model to capture the SSSI phenomena including the novel Vibrating Barrier and its effectiveness for harmonic excitation. Therefore, the adopted optimization procedure consists in minimizing the value of transfer functions $\mathrm{H}_{\boldsymbol{i}}(\boldsymbol{\alpha}, \omega)$ at the selected frequency ω_0 for each ith-structure, or if applicable, in determining the zeros of the transfer functions as conventional for tuned mass damper system (e.g. Den Hartog [32]). From Eq.(5), the optimization problem is restated as:

$$\begin{gathered} \min\{\mathrm{H_i}(\boldsymbol{\alpha}, \omega_0)\} \text{ for } i = 1, \dots, n \\ \boldsymbol{\alpha} = \left\{\mathrm{k_{ij}^V}, \eta_{\mathrm{ij}}^{\mathrm{V}}, \mathrm{m_{ii}^V}\right\} \in \mathbb{R}_0^+ \text{ for i, j} = 1, \dots, m \end{gathered} \tag{10}$$

Despite the solution of the optimization problems of Eq. (9) is usually obtained numerically, closed-form expressions can be derived in some particular cases, as described in the following section.

4. Optimal ViBa tuning for the control of two buildings

In this section, the optimal design for the ViBa parameters is obtained analytically for the case of two buildings. A simple model is used for the ViBa being defined as an internal oscillator device confined in a rigid box foundation; therefore, 2-DOFs, i.e. the internal motion of the oscillator, $\mathrm{U_{ViBa}}(\omega)$ and the displacement of its foundation, $\mathrm{U_{f,ViBa}}(\omega)$, are sufficient to describe globally the dynamic behaviour of the device. The discrete system composed of two structures protected by the Vibrating Barrier is illustrated in Fig. 2. Therefore, the governing equation of the motion Eq. (1) can be written in expanded form

$$\left\{\begin{bmatrix} \tilde{k}_1 & -\tilde{k}_1 & 0 & 0 & 0 & 0 \\ -\tilde{k}_1 & \tilde{k}_1+\tilde{k}_{f,1}+\tilde{k}_{1,2}+\tilde{k}_{1,v} & 0 & -\tilde{k}_{1,2} & 0 & -\tilde{k}_{1,v} \\ 0 & 0 & \tilde{k}_2 & -\tilde{k}_2 & 0 & 0 \\ 0 & -\tilde{k}_{1,2} & -\tilde{k}_2 & \tilde{k}_2+\tilde{k}_{f,2}+\tilde{k}_{1,2}+\tilde{k}_{2,v} & 0 & -\tilde{k}_{2,v} \\ 0 & 0 & 0 & 0 & \tilde{k}_{ViBa} & -\tilde{k}_{ViBa} \\ 0 & -\tilde{k}_{1,v} & 0 & -\tilde{k}_{2,v} & -\tilde{k}_{ViBa} & \tilde{k}_{ViBa}+\tilde{k}_{f,\mathrm{ViBa}}+\tilde{k}_{1,v}+\tilde{k}_{2,v} \end{bmatrix}\right.$$

$$\left. -\omega^2\begin{bmatrix} m_1 & 0 & 0 & 0 & 0 & 0 \\ 0 & m_{f,1} & 0 & 0 & 0 & 0 \\ 0 & 0 & m_2 & 0 & 0 & 0 \\ 0 & 0 & 0 & m_{f,2} & 0 & 0 \\ 0 & 0 & 0 & 0 & m_{ViBa} & 0 \\ 0 & 0 & 0 & 0 & 0 & m_{f,ViBa} \end{bmatrix}\right\}\begin{bmatrix} \mathrm{U}_1(\omega) \\ \mathrm{U}_{\mathrm{f},1}(\omega) \\ \mathrm{U}_2(\omega) \\ \mathrm{U}_{\mathrm{f},2}(\omega) \\ \mathrm{U}_{\mathrm{ViBa}}(\omega) \\ \mathrm{U}_{\mathrm{f,ViBa}}(\omega) \end{bmatrix} = \begin{bmatrix} 0 \\ \tilde{k}_{f,1} \\ 0 \\ \tilde{k}_{f,2} \\ 0 \\ \tilde{k}_{\mathrm{f,ViBa}} \end{bmatrix}\mathrm{U_g}(\omega)$$

(11)

Eq. (11) is easily analysed by resorting to the transfer function representation that provides a basis for determining the system response characteristics as shown in Cacciola and Tombari [3]. Therefore, the adopted procedure consists in minimizing the value of transfer functions related to the two structures, $\mathrm{H}_1(\omega)$ and $\mathrm{H}_2(\omega)$ at a selected frequency ω_0. The vector of the design parameters is reduced to $\boldsymbol{\alpha} = \{\mathrm{k_{ViBa}}, \mathrm{m_{ViBa}}, \eta_{\mathrm{ViBa}}\}$. From Eq. (10), the optimization problem is restated as:

$$\begin{gathered} \min\left\{\max\{\mathrm{H}_1(\boldsymbol{\alpha},\omega_0),\mathrm{H}_2(\boldsymbol{\alpha},\omega_0)\}\right\} \\ \boldsymbol{\alpha} = \{k_{\mathrm{ViBa}}, m_{\mathrm{ViBa}}, \eta_{\mathrm{ViBa}}\} \in \mathbb{R}_0^+ \end{gathered} \tag{12}$$

The problem in Eq.(12) can be solved by applying a numerical procedure such as the direct search method (Lagarias et al., [33]) for obtaining the optimal design parameters as done in Cacciola et al. [9].

On the other hand, a simple handy formula for tuning the ViBa is obtained after considering that the interaction with the soil is identical for the two structures (e.g. the two foundations of the buildings are identical and at the same distance); hence, the following relations occur: $\tilde{k}_f = \tilde{k}_{f,1} = \tilde{k}_{f,2}$ and $\tilde{k}_{\mathrm{SSSI}} = \tilde{k}_{1,V} = \tilde{k}_{2,V}$. Therefore, the dynamics of the problem of Eq. (11) is restated as:

$$\left\{\begin{bmatrix} \tilde{k}_1 & -\tilde{k}_1 & 0 & 0 & 0 & 0 \\ -\tilde{k}_1 & \tilde{k}_1+\tilde{k}_f+\tilde{k}_{1,2}+\tilde{k}_{\mathrm{SSSI}} & 0 & -\tilde{k}_{1,2} & 0 & -\tilde{k}_{\mathrm{SSSI}} \\ 0 & 0 & \tilde{k}_2 & -\tilde{k}_2 & 0 & 0 \\ 0 & -\tilde{k}_{1,2} & -\tilde{k}_2 & \tilde{k}_2+\tilde{k}_f+\tilde{k}_{1,2}+\tilde{k}_{\mathrm{SSSI}} & 0 & -\tilde{k}_{\mathrm{SSSI}} \\ 0 & 0 & 0 & 0 & \tilde{k}_{ViBa} & -\tilde{k}_{ViBa} \\ 0 & -\tilde{k}_{\mathrm{SSSI}} & 0 & -\tilde{k}_{\mathrm{SSSI}} & -\tilde{k}_{ViBa} & \tilde{k}_{\mathrm{ViBa}}+\tilde{k}_{f,\mathrm{ViBa}}+2\tilde{k}_{\mathrm{SSSI}} \end{bmatrix} - \omega^2 \begin{bmatrix} m_1 & 0 & 0 & 0 & 0 & 0 \\ 0 & m_{f,1} & 0 & 0 & 0 & 0 \\ 0 & 0 & m_2 & 0 & 0 & 0 \\ 0 & 0 & 0 & m_{f,2} & 0 & 0 \\ 0 & 0 & 0 & 0 & m_{ViBa} & 0 \\ 0 & 0 & 0 & 0 & 0 & m_{f,ViBa} \end{bmatrix}\right\} \begin{bmatrix} \mathrm{U}_1(\omega) \\ \mathrm{U}_{\mathrm{f},1}(\omega) \\ \mathrm{U}_2(\omega) \\ \mathrm{U}_{\mathrm{f},2}(\omega) \\ \mathrm{U}_{\mathrm{ViBa}}(\omega) \\ \mathrm{U}_{\mathrm{f,ViBa}}(\omega) \end{bmatrix} = \begin{bmatrix} 0 \\ \tilde{k}_f \\ 0 \\ \tilde{k}_f \\ 0 \\ \tilde{k}_{\mathrm{f,ViBa}} \end{bmatrix} \mathrm{U}_{\mathrm{g}}(\omega) \tag{13}$$

Similarly, Eq. (13) is analysed by resorting to the transfer function; the optimisation procedure consists in obtaining the minimum of the structural responses by considering the vector of the design parameters as $\boldsymbol{\alpha} = \{\mathrm{k}_{\mathrm{ViBa}}, \mathrm{m}_{\mathrm{ViBa}}, \eta_{\mathrm{ViBa}}\}$.

Clearly, the solution of the optimization problem is straightforward when the value of a single unknown can be assigned *a priori*. It is noted that the mass of the ViBa $\mathrm{m}_{\mathrm{ViBa}}$ is restrained by engineering criteria (e.g. bearing capacity of the soil, volumetric restraint, etc...). Therefore, by assigning $\mathrm{m}_{\mathrm{ViBa}}$ as a known quantity, the optimal value of the stiffness, $k_{\mathrm{ViBa}}^{\mathrm{optimal}}$, and the optimal value of the loss factor, $\eta_{\mathrm{ViBa}}^{\mathrm{optimal}}$, are derived in closed form by determining the zeros of the transfer functions $\mathrm{H}_1(\boldsymbol{\alpha}, \omega_0)$ and $\mathrm{H}_2(\boldsymbol{\alpha}, \omega_0)$, derived from Eq. (9) as follows:

$$\begin{cases} \mathrm{H}_1(\boldsymbol{\alpha}, \omega_0) = 0 \\ \mathrm{H}_2(\boldsymbol{\alpha}, \omega_0) = 0 \end{cases} \tag{14}$$

It is noted that both numerators of the equations in Eq. (14) can be written as the product of two functions in the following form:

$$\begin{cases} \mathrm{f}(\boldsymbol{\alpha}, \omega_0)\mathrm{g}_1(\omega_0) = 0 \\ \mathrm{f}(\boldsymbol{\alpha}, \omega_0)\mathrm{g}_2(\omega_0) = 0 \end{cases} \tag{15}$$

where each expression is separated into two components: $\mathrm{g}_1(\omega_0)$ and $\mathrm{g}_2(\omega_0)$ depending on the characteristics of the buildings, foundation and soil-interaction whereas $\mathrm{f}(\boldsymbol{\alpha}, \omega_0)$, noticeably identical in both expressions, is as a function of the ViBa parameters as defined below:

$$\begin{aligned}\mathrm{f}(\boldsymbol{\alpha}, \omega_0) = \tilde{k}_{\mathrm{ViBa}}(\omega_0)\left[\tilde{k}_{\mathrm{f,ViBa}} + \tilde{k}_{\mathrm{SSSI}}\left(2 + \frac{\tilde{k}_{\mathrm{f,ViBa}}}{\tilde{k}_{\mathrm{f}}}\right) - \omega_0^2\left(m_{\mathrm{f,ViBa}} + m_{\mathrm{ViBa}}\right)\right] \\ - (\omega_0^2 \mathrm{m}_{\mathrm{ViBa}})\left[\tilde{k}_{\mathrm{f,ViBa}} + \tilde{k}_{\mathrm{SSSI}}\left(2 + \frac{\tilde{k}_{\mathrm{f,ViBa}}}{\tilde{k}_{\mathrm{f}}}\right) - \omega_0^2 m_{\mathrm{f,ViBa}}\right]\end{aligned} \tag{16}$$

By setting to zero Eq. (16), the optimal value of the ViBa complex stiffness, $\tilde{k}_{\mathrm{ViBa}}^{\mathrm{optimal}}$, is obtained:

$$\tilde{k}_{\mathrm{ViBa}}^{\mathrm{optimal}}(\omega_0) = \frac{(\omega_0^2 \mathrm{m}_{\mathrm{ViBa}})\left[\tilde{k}_{\mathrm{f,ViBa}} + \tilde{k}_{\mathrm{SSSI}}\left(2 + \frac{\tilde{k}_{\mathrm{f,ViBa}}}{\tilde{k}_{\mathrm{f}}}\right) - \omega_0^2 m_{\mathrm{f,ViBa}}\right]}{\tilde{k}_{\mathrm{f,ViBa}} + \tilde{k}_{\mathrm{SSSI}}\left(2 + \frac{\tilde{k}_{\mathrm{f,ViBa}}}{\tilde{k}_{\mathrm{f}}}\right) - \omega_0^2\left(m_{\mathrm{f,ViBa}} + m_{\mathrm{ViBa}}\right)} \tag{17}$$

Therefore, following Eq. (17), the stiffness $k_{\mathrm{ViBa}}^{\mathrm{optimal}}$ and the damping $\eta_{\mathrm{ViBa}}^{\mathrm{optimal}}$ are derived as follows:

$$\begin{aligned} k_{\mathrm{ViBa}}^{\mathrm{optimal}} &= \mathrm{Re}\left\{\tilde{k}_{\mathrm{ViBa}}^{\mathrm{optimal}}(\omega_0)\right\} \\ \eta_{\mathrm{ViBa}}^{\mathrm{optimal}} &= \frac{\mathrm{Im}\left\{\tilde{k}_{\mathrm{ViBa}}^{\mathrm{optimal}}(\omega_0)\right\}}{\mathrm{Re}\left\{\tilde{k}_{\mathrm{ViBa}}^{\mathrm{optimal}}(\omega_0)\right\}} \end{aligned} \tag{18}$$

where $\mathrm{Re}\{\cdot\}$ and $\mathrm{Im}\{\cdot\}$ indicate the real and imaginary component of complex value $\tilde{k}_{\mathrm{ViBa}}^{\mathrm{optimal}}$. Therefore, Eq. (18) is used to tune the Vibrating Barrier for mitigating the dynamic response of both two buildings. It is worth noting that Eq. (17) depends neither on the structural characteristics of the buildings nor on the interaction between them. Clearly if ω_0 is selected as first natural frequency of either one of the two buildings the structural characteristics are implicitly embedded in ω_0, however it is noted that this might not be necessary the best option whereas the fundamental soil frequency plays a relevant role in the dynamic response

of the system. Also, despite the rather strong assumption made for obtaining the analytical formula (e.g. the two foundations of the buildings are identical and at the same distance), Eq. (17) can be used as starting point of the nonlinear optimization procedure of Eq.(12) as done in the section 5.2.

5. Numerical and Experimental Results

In this section, numerical and experimental analyses are carried out to investigate the performance of the Vibrating Barrier to reduce the vibrations of a cluster of two structures, (i.e. Structure 1 and Structure 2), subjected to ground motion excitation. The physical model is represented by the prototype depicted in Fig. 3 where silicone rubber is used to mimic the soil behaviour; mechanical properties of each element used in the prototype are reported in Table 1.

In order to understand the efficiency of the ViBa, parametric analyses accounting for various ViBa mass ($\mathrm{m_{ViBa}}$), damping values (η_{ViBa}), as well as the stiffness of the structure-soil-structure interaction, $k_{1,2}$, are initially performed by using the analytical formula of Eq. (17); moreover, experimental shake table tests of the physical model of Fig. 3 are carried out for validation process.

Steady-state analyses are performed for both cases without and with the protection offered by the ViBa; the Vibrating Barrier is tuned to reduce the vibrations induced by an harmonic input at the frequency $\mathrm{f_0} = 10.6$ Hz (i.e. $\omega_0 = 66.57$ rad/s), corresponding to the first natural frequency of Structure 1, by resorting to the optimization formula described in Eq. (17). Results are presented in terms of modulus of transfer function and index of reduction calculated as

$$\mathrm{I_R} = 1 - |\mathrm{H_i}(\omega_0)|/|\mathrm{H}_i^{unc}(\omega_0)| \text{ for } i = 1,2 \tag{19}$$

where $\mathrm{H}_i^{unc}(\omega_0)$ is the steady state response of the structure without being protected by the ViBa device pertinent to the structural degree of freedom $\mathrm{U_i}$,with $i = 1,2$, as shown in Fig. 2 at the selected frequency ω_0.

It is worth noting that the index of reduction, although appropriate to capture the performance of the ViBa at a single frequency (see e.g. Woods [1]) might not be appropriate for representing the global behaviour of the system under broad-band excitation for which alternative measures and approaches need to be used (e.g. see [8-10]).

Finally, the influence of the position of the ViBa with respect to the two structures calibrated through the numerical procedure of Eq. (12) is analysed and verified by adopting a finite element model.

5.1 Numerical results for a cluster of buildings with identical soil interaction

The efficiency of the Vibrating Barrier (ViBa) for mitigating the dynamic response of a cluster of building is applied to the discrete system of Fig. 2; the values of the components used for populating the matrices of the governing equation written in Eq. (13) are derived according to the prototype of Structure-ViBa-Structure interaction depicted in Fig. 3. The values used in the following parametric analyses are reported in Table 2.

Fig. 4a-b shows the modulus of the transfer function responses of Structure 1 and Structure 2, respectively, when equal structural characteristics are considered; the curve related to the case without the ViBa is compared to the dynamic responses of the buildings with the protection of the ViBa, obtained by calibrating its stiffness, $k_{\mathrm{ViBa}}^{\mathrm{optimal}}$, for three different mass ratios $m_{ViBa}/m_{str} = \{0.5; 1.0; 1.5\}$ with respect to the structural masses, where $m_{str} = m_1 = m_2$. The results, clearly identical for Structure 1 and Structure 2, show the mitigation of the structural response at the design frequency $\mathrm{f_0} = 10.6$ Hz. As already observed in Cacciola

and Tombari [3] for the case of a single building, the extent of the reduction increases with the increase of the mass ratio in case of damped system; for the case of two buildings, a reduction ranging from $\mathrm{I_R}$=75.18% ($^{m_{ViBa}}/_{m_{str}} = 0.5$) to $\mathrm{I_R}$=91.00% ($^{m_{ViBa}}/_{m_{str}} = 1.5$) is obtained for both structures. The dynamic response of each degree of freedom of Fig. 2 in terms of absolute displacement transfer function in case of $^{m_{ViBa}}/_{m_{str}} = 1$ is depicted in Fig. 5.

In Fig. 6a-b the characteristics of Structure 2 is altered in order to simulate a scenario where the ViBa protects buildings with different properties, hence Structure 2 height is reduced of 30% to obtain a stiffer ($k_2 = 5.6603 \times 10^3$ N/m, frequency at the peak 12.37 Hz) building. The ViBa barrier is tuned exactly as the previous case since, as already mentioned, Eq. (12) is independent from the characteristics of the superstructure. The transfer functions related to Structure 1 show slight deviations from the previously obtained due to the different structure-soil-structure interaction; on the other hand, the transfer functions due to Structure 2 are changed due to the different structural characteristics. It is worth emphasizing that despite the different global responses, the same reduction ranging from $\mathrm{I_R}$=71.90% ($^{m_{ViBa}}/_{m_{str}} = 0.5$) to $\mathrm{I_R}$=90.27% ($^{m_{ViBa}}/_{m_{str}} = 1.5$) is achieved for both structures at the selected frequency. The dynamic response of each degree of freedom of Fig. 2 in terms of absolute displacement transfer function in case of $^{m_{ViBa}}/_{m_{str}} = 1$ is depicted in Fig. 7.

Furthermore, an increment of the ViBa damping, $\eta_{\mathrm{ViBa}} > \eta_{\mathrm{ViBa}}^{\mathrm{optimal}}$, will decrease the maximum reduction to the harmonic input but on the other hand will improve the efficiency of the ViBa for broadband signals. Fig. 8a-b show the steady state response of both structures by moving the damping of the ViBa far away the optimal value; in the case of η_{ViBa}=0.05, the global response results decreased with respect to the scenario without ViBa while the reduction at the frequency of $\mathrm{f_0} = 10.6$ Hz decrease with the increase of the damping.

Finally, Fig. 9a-b show the independence of the tuning formula from the interaction between the two structures. Steady-state responses are drawn for different value of $k_{1,2}$ with respect

to $k_{1,2}^{0} = 50$ N/m adopted for the previous cases; although the global responses are different, a minimum occurs in both analyses at the frequency of $f_0 = 10.6$ Hz, and the I_R= 85% is achieved.

5.2 Shake table testing results for two buildings with identical soil interaction

In this section, the proposed optimization procedure for tuning the Vibrating Barrier (ViBa) parameters is applied to investigate the dynamic response of the investigated problem consisting of two buildings, Structure 1 and Structure 2, supported on embedded mat foundations. The prototype with equal and different buildings, as illustrated in Fig. 10 respectively, is realized in order to carry out experimental shake table tests to validate the numerical results obtained through the finite element method. The ground soil is defined by a linear visco-elastic material, reproduced by silicone rubber (Niwa et al. [28], Kitada et al. [29] and Cacciola et al., [9]). Buildings are realized as single-story structures with aluminium structural walls of rectangular cross section of 40 mm width and 0.12 mm thick and an acrylic roof with an added mass of 0.1 kg. The characteristics of the materials used in the numerical analysis are reported in Table 1. Structure 1 is 170 mm high; this value is kept as constant for every test performed in this paper while the height of the Structure 2 changes according the values reported in Table 4. In particular, three different case studies are investigated: protection of structures with identical characteristics, named as Case Study A, protection of structures with different characteristics, referred to as Case Study B and Case Study C according to the two design frequency used for tuning the ViBa.

The Vibrating Barrier is modelled as a single oscillator consisting of mass placed in a sliding tray on a rack and springs connected to the embedded box foundation. The damping of the ViBa, η_{ViBa}, is equal to 0.04 as estimated by an identification procedure (i.e. best fit of numerical and experimental evaluated transfer functions).

The aim of the study is to reduce the maximum accelerations of both Structure 1 and Structure 2 at a design frequency. Experimental shake table testing is performed by applied

harmonic accelerations at the base with input frequency ranging from 5 to 15 Hz; the results are obtained in terms of frequency response functions by normalizing the Fourier Transform of the accelerations recorded at the top of each building by the Fourier Transform of the input signal applied at the base.

Moreover, the described experiments are further validated by positive comparison with those obtained by numerical simulation of a pertinent finite element model.

5.2.1 Case Study A

The first case study (Case study A) investigates a scenario with two identical structures. In order to protect them from ground motions, a Vibrating Barrier (ViBa) device is embedded into the soil between the two structures (see Fig. 4) at the relative distance of 40 mm from each building. The ViBa is tuned in order to protect the structures at the frequency ω_0 corresponding to the “resonant” or first natural frequency of both buildings in the existing situation. The soil interaction stiffness coefficients are derived by conventional numerical technique such as the matrix stiffness method since the soil behaviour is assumed linear elastic. The elastic component of the ViBa is simulated by means of a two-joint link while a lumped mass is assigned to a free node place at the end of the link. The internal damping of the ViBa, η_{ViBa}, is experimentally determined from the prototype as equal to 0.04. This value is greater than the ideal optimal value $\eta_{\mathrm{ViBa}} = 0$ determined numerically by using the design procedure proposed in this paper in Eq. (17) and Eq. (18); the design values used in this case are reported in Table 3.

Experimental steady state analyses are carried out for both scenarios of structures without and with protection of the ViBa. Harmonic signals with input frequency ranging from 5 to 15 Hz are applied at the base of the prototype. The maximum acceleration recorded at the top of the structure for each harmonic signal normalized by the maximum acceleration of the input signal represents the ordinate of the transfer function at the given frequency, as illustrated in Fig. 14a-b for Structure 1 and Structure 2, respectively. Moreover, the results

are compared to the numerical model proposed in Fig. 11 showing a good matching between numerical and experimental results.

It is worth noting that the two structural responses are the same since the two buildings are equal. Moreover, the ViBa strongly reduces the structural response at the design input frequency of 10.6 Hz where the resonance of the structures is expected; by using the ViBa, a relevant reduction of 46.2% of the maximum acceleration for both Structure 1 and Structure 2 is accomplished.

5.2.2 Case Study B

In the Case Study B, Structure 1 is kept as same as the case study A whereas Structure 2 has an reduced height of 0.16 m, as illustrated in Fig. 17. Therefore, this case aims to investigate the performance of the ViBa when buildings with different natural frequency are located within the ViBa area of influence (e.g. see [9] and [34]).

Since there are two different frequencies of interest, namely the natural frequency of the Structure 1 at 10.6 Hz and the natural frequency of Structure 2 at 11.3 Hz, which both can lead to relevant damages to the buildings, a design consideration should be firstly done; in Case Study B, the effect on the global system when the ViBa is tuned at the fundamental frequency of Structure 2, $f_0 = 11.3$ Hz, is investigated. Design values are reported in Table 3.

Experimental steady state analyses are performed with and without the coupling with the ViBa device assigning harmonic input ranging from 5Hz to 15Hz. Independently, numerical analyses are performed through the model depicted in Fig. 12 for the same case.

Results in terms of absolute structural acceleration in the frequency domain are reported in Fig. 16a-b for both Structure 1 and Structure 2, respectively. For the design harmonic input at the frequency 11.3 Hz, a reduction of about 38.4% of the maximum acceleration is accomplished for the target Structure 2. A similar reduction of 36.71% is obtained for Structure 1 at the design frequency of 11.3 Hz.

Nevertheless, the acceleration at the fundamental frequency of Structure 1 is increased of 31.2%. This behaviour occurs when the ViBa is tuned at the frequency higher than the natural frequency of the building. It is worth pointing out that in case of narrow-band signals, this behaviour does not produce any detrimental effects; nevertheless, a different strategy for the choice of the design frequency ω_0 should be taken for accomplishing the reduction for both buildings as done for the following Case Study C below.

5.2.3 Case Study C

Case Study C investigates the set-up done for Case Study B, i.e. scenario with different structures as illustrated in Fig. 17, but a different choice is made for tuning the ViBa in order to accomplish the reduction for both buildings. It is worth noting that the tuning formula of Eq. (17) is independent of the structural characteristics. Therefore, the parameters of the ViBa are the same obtained for the Case Study A where the same design frequency ω_0 was used. This is noteworthy since the performance of the ViBa is still effective even if buildings will be modified onwards.

Experimental steady state analyses are performed for both scenarios, of structures without and with protection of the ViBa, as previously carried out. The structural response in acceleration in the frequency domain is reported in Fig. 18. For the harmonic input at the frequency 10.6 Hz, corresponding to the natural frequency of the Structure 1, still relevant reductions are recorded; reduction over 47.9% of the maximum acceleration is accomplished for Structure 1 by using the ViBa. The beneficial effects are obtained even for Structure 2 where it is achieved a relevant reduction of 44% at the working frequency of the ViBa at 10.6 Hz; furthermore, a slightly reduction is observed at the resonance frequency of Structure 2 being reduced of about 15.3% without being tuned for it.

Finally, it is worth mentioning that the trench realized for containing the ViBa slightly alters the natural frequencies of the buildings due to the alteration of the structure-soil-structure interaction caused by the excavation, as reported in Table 4 and showed in Fig. 13; in particular, the effect is more marked when the two structures are different. Therefore, ViBa

needs to be tuned by considering this shift in frequency. Furthermore, this manifests clearly the role of the vibrating component of the ViBa in comparison of the static counterpart (i.e. the trench realized to embed the ViBa) that slightly alters the structural frequency response by increasing the soil stiffness.

5.3 Numerical analyses for a cluster of buildings with different soil interactions

Finally, in this section the influence of the position of the ViBa is analysed. By considering the buildings of the Case Study A, two different scenarios are modelled in Fig. 19 where the ViBa is placed in line with the structures at two difference distances from the buildings. Since the assumptions made for the analytical formula in Eq. (17) are not satisfied due to the different soil-foundation and soil-ViBa interaction for each building, the numerical procedure of Eq. (12) is used.

After applying the direct stiffness method in order to calibrate the stiffness values of the discrete model of Fig. 2, the minimization problem is solved for $m_{ViBa} = 0.7\ kg$ providing the optimal value of $k_{\mathrm{ViBa}} = 3257.53\ N/m$ for the Case Study 1 of Fig. 19a and of $k_{\mathrm{ViBa}} = 3278.18\ N/m$ for the Case Study 2 of Fig. 19b for controlling an harmonic input at the target frequency of $\omega_0 = 10.7$ Hz.

Results of the steady-state analysis for both buildings in the Case Study 1 and Case Study 2 are shown in Fig. 20 and Fig. 21, respectively. The responses show that the higher is the distance between ViBa and buildings the lesser is the influence of the ViBa; nevertheless, beneficial effects are manifested in both structures.

6. Concluding Remarks

The paper presents a simplified discrete model to capture the structure-soil-structure interaction between two adjacent buildings and the novel Vibrating Barrier (ViBa) device. A closed-form solution for tuning the ViBa parameters is established for the case of two

buildings with identical soil-ViBa and soil-foundation interaction forced by harmonic excitation.

A numerical finite element model is also realized by considering both cases of structures with and without the Vibrating Barrier to consider most general cases.

Parametric analyses are performed to evaluate the influence of the ViBa on the dynamic response of the two buildings and its beneficial effect through a simple optimization scheme. Specifically, relevant reductions of over 70% and up to 90% (at the target frequency) of the maximum harmonic acceleration are achieved. Moreover, beneficial effects have been observed for both structures in every investigated case when the ViBa is properly designed.

Results have been validated by experimental shake table tests on a prototype with two equal and different structures founded on silicone rubber specimen simulating the soil. An excellent matching between numerical and experimental results is obtained, showing the ability of the proposed discrete model to capture this complex phenomenon. Furthermore, reduction up to 46.2% of the maximum acceleration for both Structure 1 and Structure 2 is accomplished experimentally.

Although the presented work has been focused on the harmonic response of a cluster of structures protected by the novel device ViBa, it has to be emphasized that in case of more general broad-band signals such as a seismic excitation, not dealt with in this paper, the Vibrating Barrier has to be properly tuned in order to avoid detrimental effects by extending to a cluster of buildings the optimization criteria proposed in Cacciola et al. [9] for a single building.

References

[1]R. D. Woods, “Screening of surface waves in soils,” J. Soil Mech. Found. Eng. Div., vol. 94, no. 4, pp. 951–979, 1968.
[2]A. Colombi, D. Colquitt, P. Roux, S. Guenneau, and R. V. Craster, “A seismic metamaterial: The resonant metawedge,” Scientific Reports, vol. 6, p. 27717, Jun. 2016.
[3]G. Finocchio et al., “Seismic metamaterials based on isochronous mechanical oscillators,” Applied Physics Letters, vol. 104, no. 19, p. 191903, May 2014.
[4]S. Krödel, N. Thomé, and C. Daraio, “Wide band-gap seismic metastructures,” Extreme Mechanics Letters, vol. 4, pp. 111–117, Sep. 2015.
[5]P. R. Wagner, V. K. Dertimanis, I. A. Antoniadis, and E. N. Chatzi, “On the feasibility of structural metamaterials for seismic-induced vibration mitigation,” International Journal of Earthquake and Impact Engineering, vol. 1, no. 1/2, p. 20, 2016.
[6]V. K. Dertimanis, I. A. Antoniadis, and E. N. Chatzi, “Feasibility Analysis on the Attenuation of Strong Ground Motions Using Finite Periodic Lattices of Mass-in-Mass Barriers,” Journal of Engineering Mechanics, vol. 142, no. 9, p. 04016060, Sep. 2016.
[7]A. Palermo, S. Krödel, A. Marzani, and C. Daraio, “Engineered metabarrier as shield from seismic surface waves,” Scientific Reports, vol. 6, no. 1, Dec. 2016.
[8]P. Cacciola and A. Tombari, “Vibrating barrier: a novel device for the passive control of structures under ground motion,” Proceedings of the Royal Society of London A: Mathematical, Physical and Engineering Sciences, vol. 471, no. 2179, Jul. 2015.
[9]P. Cacciola, M. G. Espinosa, and A. Tombari, “Vibration control of piled-structures through structure-soil-structure-interaction,” Soil Dynamics and Earthquake Engineering, vol. 77, pp. 47–57, Oct. 2015.
[10]A. Tombari, I. Zentner, and P. Cacciola, “Sensitivity of the stochastic response of structures coupled with vibrating barriers,” Probabilistic Engineering Mechanics, vol. 44, pp. 183–193, Apr. 2016.
[11]D. Clouteau and D. Aubry, “Modifications of the Ground Motion in Dense Urban Areas,” Journal of Computational Acoustics, vol. 09, no. 04, pp. 1659–1675, Dec. 2001.
[12]F. J. Chávez-García and M. Cárdenas, “The contribution of the built environment to the ‘free-field’ ground motion in Mexico City,” Soil Dynamics and Earthquake Engineering, vol. 22, no. 9–12, pp. 773–780, Oct. 2002.
[13]P. Guéguen, P.-Y. Bard, and F. Chavez-Garcia, “Site-City Interaction in Mexico City-Like environments: An Analytical Study,” Bulletin of the Seismological Society of America, vol. 92, no. 2, pp. 794–811, 2002.
[14]M. Kham, J.-F. Semblat, P.-Y. Bard, and P. Dangla, “Seismic Site-City Interaction: Main Governing Phenomena through Simplified Numerical Models,” Bulletin of the Seismological Society of America, vol. 96, no. 5, pp. 1934–1951, Oct. 2006.
[15]M. Ghergu and I. R. Ionescu, “Structure–soil–structure coupling in seismic excitation and ‘city effect,’” International Journal of Engineering Science, vol. 47, no. 3, pp. 342–354, Mar. 2009.
[16]Y. Isbiliroglu, R. Taborda, and J. Bielak, “Coupled Soil-Structure Interaction Effects of Building Clusters During Earthquakes,” Earthquake Spectra, vol. 31, no. 1, pp. 463–500, Feb. 2015.
[17]L. Schwan, C. Boutin, L. A. Padrón, M. S. Dietz, P.-Y. Bard, and C. Taylor, “Site-city interaction: theoretical, numerical and experimental crossed-analysis,” Geophysical Journal International, vol. 205, no. 2, pp. 1006–1031, May 2016.
[18]P. Gueguen and A. Colombi, “Experimental and Numerical Evidence of the Clustering Effect of Structures on Their Response during an Earthquake: A Case Study of Three

Identical Towers in the City of Grenoble, France," Bulletin of the Seismological Society of America, vol. 106, no. 6, pp. 2855–2864, Dec. 2016.
[19]G. B. Warburton, J. D. Richardson, and J. J. Webster, "Forced Vibrations of Two Masses on an Elastic Half Space," Journal of Applied Mechanics, vol. 38, no. 1, p. 148, 1971.
[20]J. E. Luco and L. Contesse, "Dynamic structure-soil-structure interaction," Bulletin of the Seismological Society of America, vol. 63, no. 4, pp. 1289–1303, Aug. 1973.
[21]H. L. Wong and M. D. Trifunac, "Two-dimensional, antiplane, building-soil-building interaction for two or more buildings and for incident planet SH waves," Bulletin of the Seismological Society of America, vol. 65, no. 6, pp. 1863–1885, 1975.
[22]M. Lou, H. Wang, X. Chen, and Y. Zhai, "Structure–soil–structure interaction: Literature review," Soil Dynamics and Earthquake Engineering, vol. 31, no. 12, pp. 1724–1731, Dec. 2011.
[23]T. Kobori, Minai, Ryoichiro, and Kusakabe, Kaoru, "Dynamical Characteristics of Soil-Structure Cross-Interaction System, I," Bulletin of the Disaster Prevention Research Institute, vol. 22, no. 2, pp. 111–151, 1973.
[24]J. S. Mulliken and D. L. Karabalis, "Discrete model for dynamic through-the-soil coupling of 3-D foundations and structures," Earthquake Engineering & Structural Dynamics, vol. 27, no. 7, pp. 687–710, Jul. 1998.
[25]N. A. Alexander, E. Ibraim, and H. Aldaikh, "A simple discrete model for interaction of adjacent buildings during earthquakes," Computers & Structures, vol. 124, pp. 1–10, Aug. 2013.
[26]H. Aldaikh, N. A. Alexander, E. Ibraim, and O. Oddbjornsson, "Two dimensional numerical and experimental models for the study of structure–soil–structure interaction involving three buildings," Computers & Structures, vol. 150, pp. 79–91, Apr. 2015.
[27]H. Aldaikh, N. A. Alexander, E. Ibraim, and J. Knappett, "Shake table testing of the dynamic interaction between two and three adjacent buildings (SSSI)," Soil Dynamics and Earthquake Engineering, vol. 89, pp. 219–232, Oct. 2016.
[28]M. Niwa, K. Ueno, K. Yahata, and T. Ishibashi, "Vibration tests of soil-structure interaction using silicone rubber soil model," in Ninth World Conference on Earthquake Engineering, Tokyo-Kyoto, Japan, 1988.
[29]Y. Kitada, T. Hirotani, and M. Iguchi, "Models test on dynamic structure–structure interaction of nuclear power plant buildings," Nuclear Engineering and Design, vol. 192, no. 2–3, pp. 205–216, Sep. 1999.
[30]S. L. Kramer, Geotechnical earthquake engineering. Upper Saddle River, N.J.: Prentice Hall, 1996.
[31]A. A. Chanerley and N. A. Alexander, "Obtaining estimates of the low-frequency 'fling', instrument tilts and displacement timeseries using wavelet decomposition," Bulletin of Earthquake Engineering, vol. 8, no. 2, pp. 231–255, Apr. 2010.
[32]J. P. Den Hartog, Mechanical vibrations. New York: Dover Publications, 1985.
[33]J. C. Lagarias, J. A. Reeds, M. H. Wright, and P. E. Wright, "Convergence Properties of the Nelder--Mead Simplex Method in Low Dimensions," SIAM Journal on Optimization, vol. 9, no. 1, pp. 112–147, Jan. 1998.
[34]P. Cacciola, A. Tombari, and I. Zentner, "Vibration control of an industrial building through the vibrating barrier," in Conference: Earthquake Risk and Engineering towards a Resilient World, Cambridge, UK, 2015.

ALL FIGURES ARE IN COLOUR IN THE ONLINE VERSION ONLY

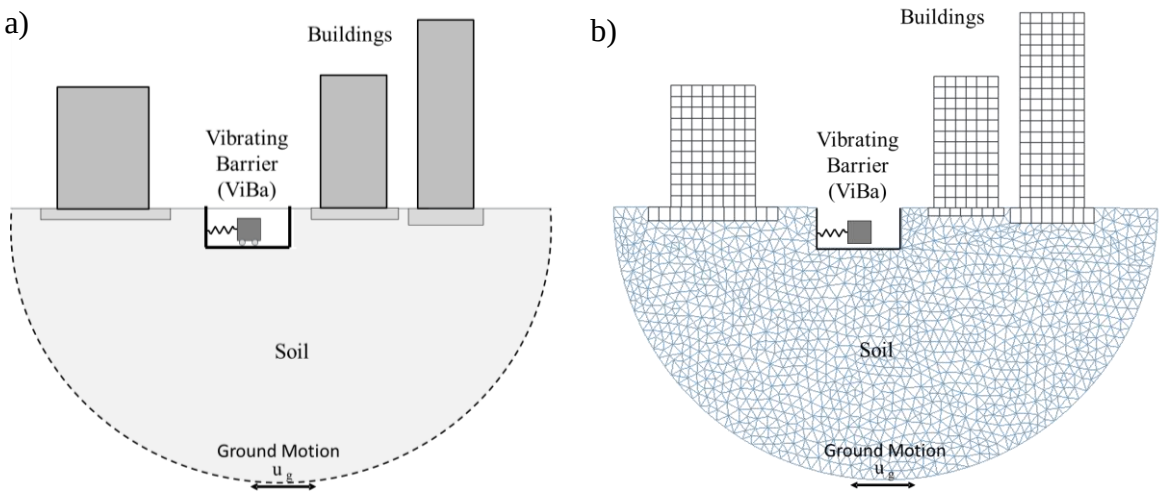

Fig. 1 Vibrating Barrier (ViBa) device embedded in the soil for protecting a cluster of buildings: a) continuous model; b) Finite Element model.

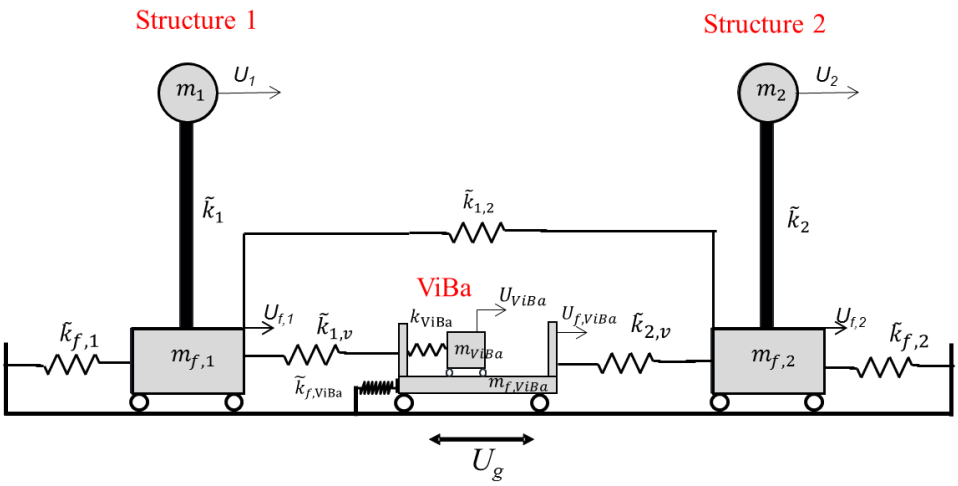

Fig. 2 Simplified mechanical model of two structures protected by the ViBa device.

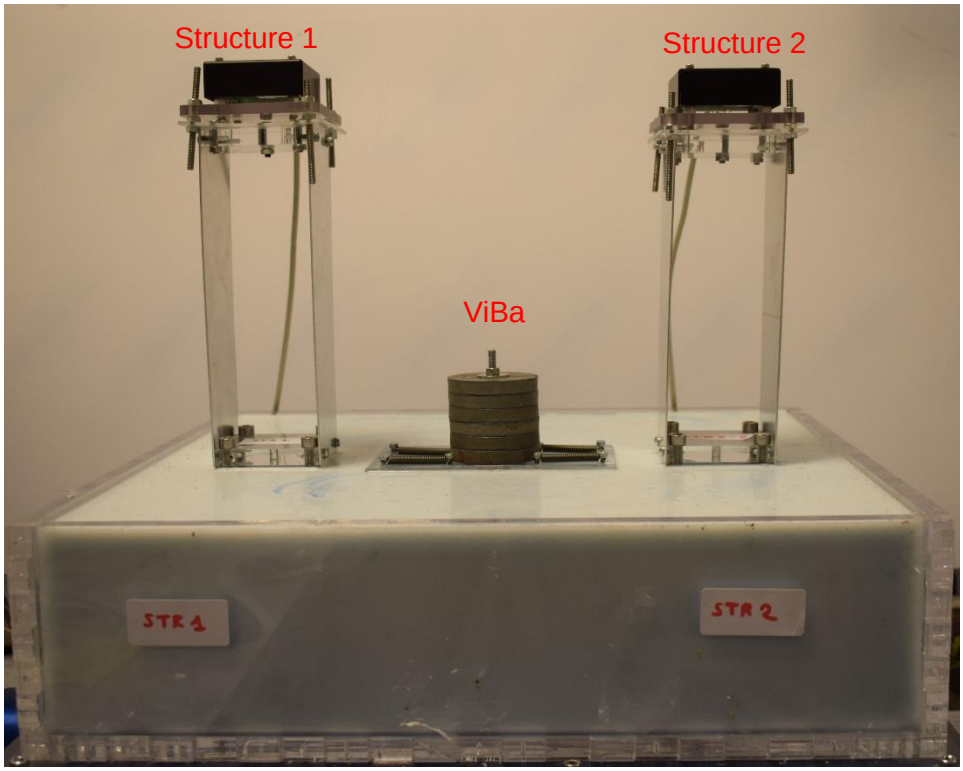

Fig. 3 Study Case: ViBa protecting a cluster of two buildings.

Table 1 Properties of the materials used in the model

Element	Material	Elastic modulus [kPa]	Poisson coefficient	Unit weight (kN/m^3)
Soil	Silicone Rubber	470.66	0.47	12.29
Structural walls	Aluminium	69637055	0.33	26.61
Foundation/roof	Acrylic	2452000	0.35	11.67

Table 2 Parameters used to describe the discrete system representing the cluster of buildings protected by the ViBa device

		[N/m]				[kg]		
$\boldsymbol{k_1}$	k_2	1.9415e+03	Var.	m_1	m_2	0.185	η_{str}	0.02
$\boldsymbol{k_{f,1}}$	$k_{f,1}$	1.5767e+03		$m_{f,1}$	$m_{f,2}$	0.04	$\eta_{\mathrm{f,str}}$	0.1
$\boldsymbol{k_{\mathrm{SSSI}}}$		1.0362e+03		$m_{f,ViBa}$		0.09	η_{SSSI}	0.0
$\boldsymbol{k_{f,\mathrm{ViBa}}}$		1.4607e+04		m_{ViBa}		0.7	$\eta_{\mathrm{f,ViBa}}$	0.1
$\boldsymbol{k_{1,2}}$		50					$\eta_{1,2}$	0.0

Table 3 Design Parameters used to tune the Vibrating Barrier for the three cases

	Case Study A	Case Study B	Case Study C
k_{ViBa}	3080 N/m	3080 N/m	3080 N/m
m_{ViBa}	0.7 kg	0.615 kg	0.7 kg
η_{ViBa}	0.04	0.04	0.04

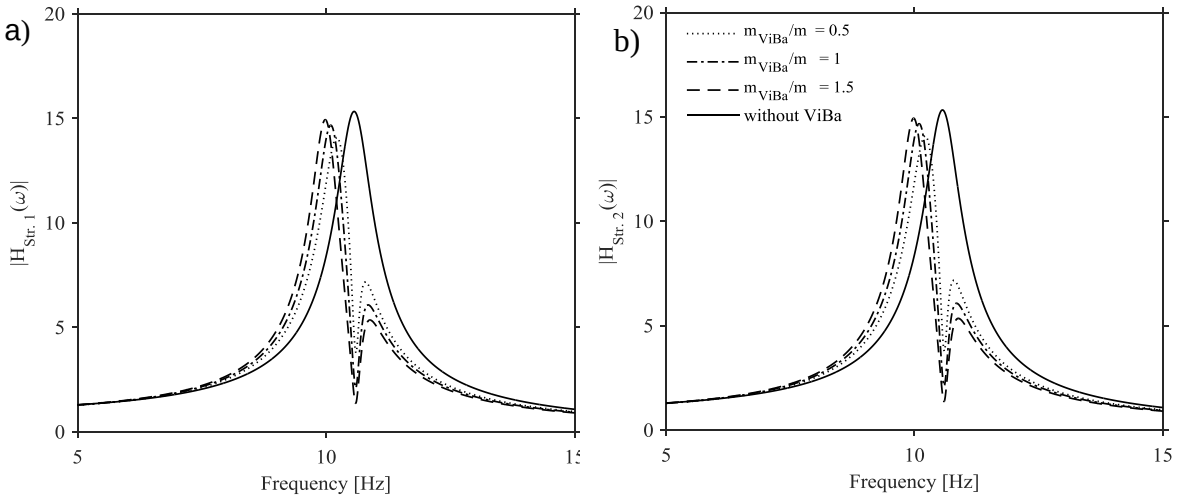

Fig. 4 Module of the transfer functions of a) Structure 1 and b) Structure 2 with equal characteristics for different values of the mass of the ViBa.

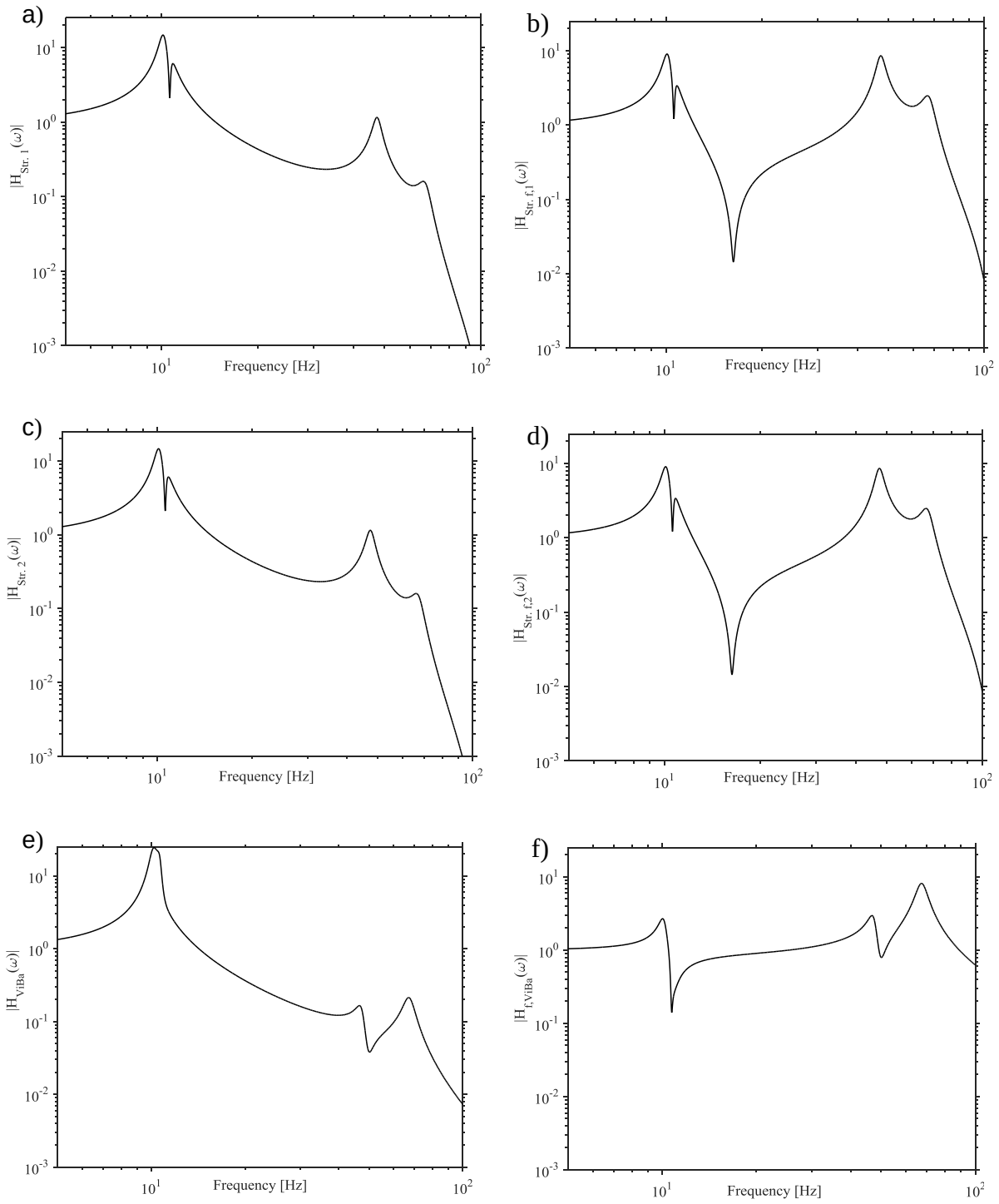

Fig. 5 Module of the transfer functions in logarithmic scale of the case with identical structures coupled with ViBa for every degree of freedom: a) Structure 1, b) foundation 1, c) Structure 2 and d) foundation 2, e) VIBa and b) ViBa foundation.

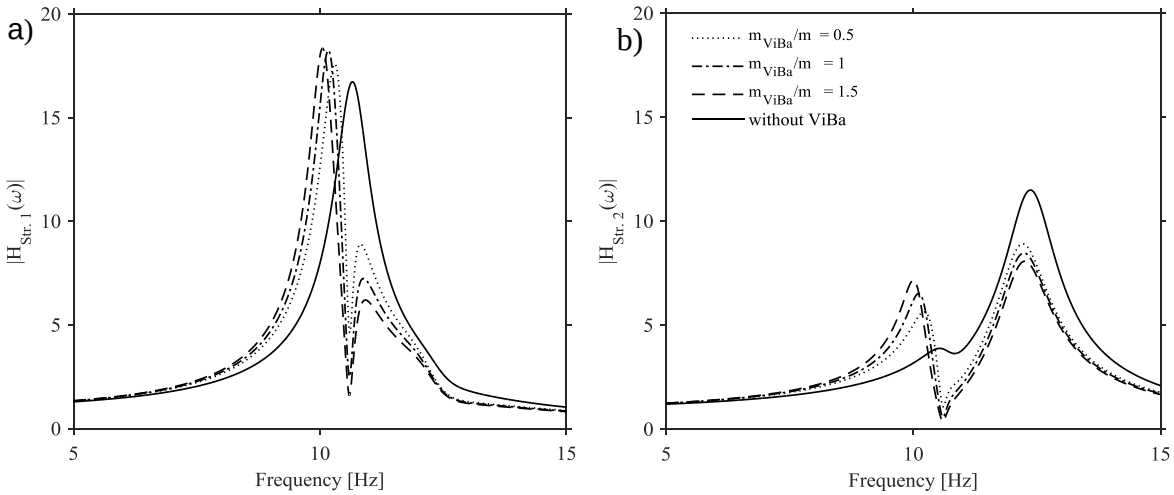

Fig. 6 Module of the transfer functions of a) Structure 1 and b) Structure 2 with different characteristics for different values of the mass of the ViBa.

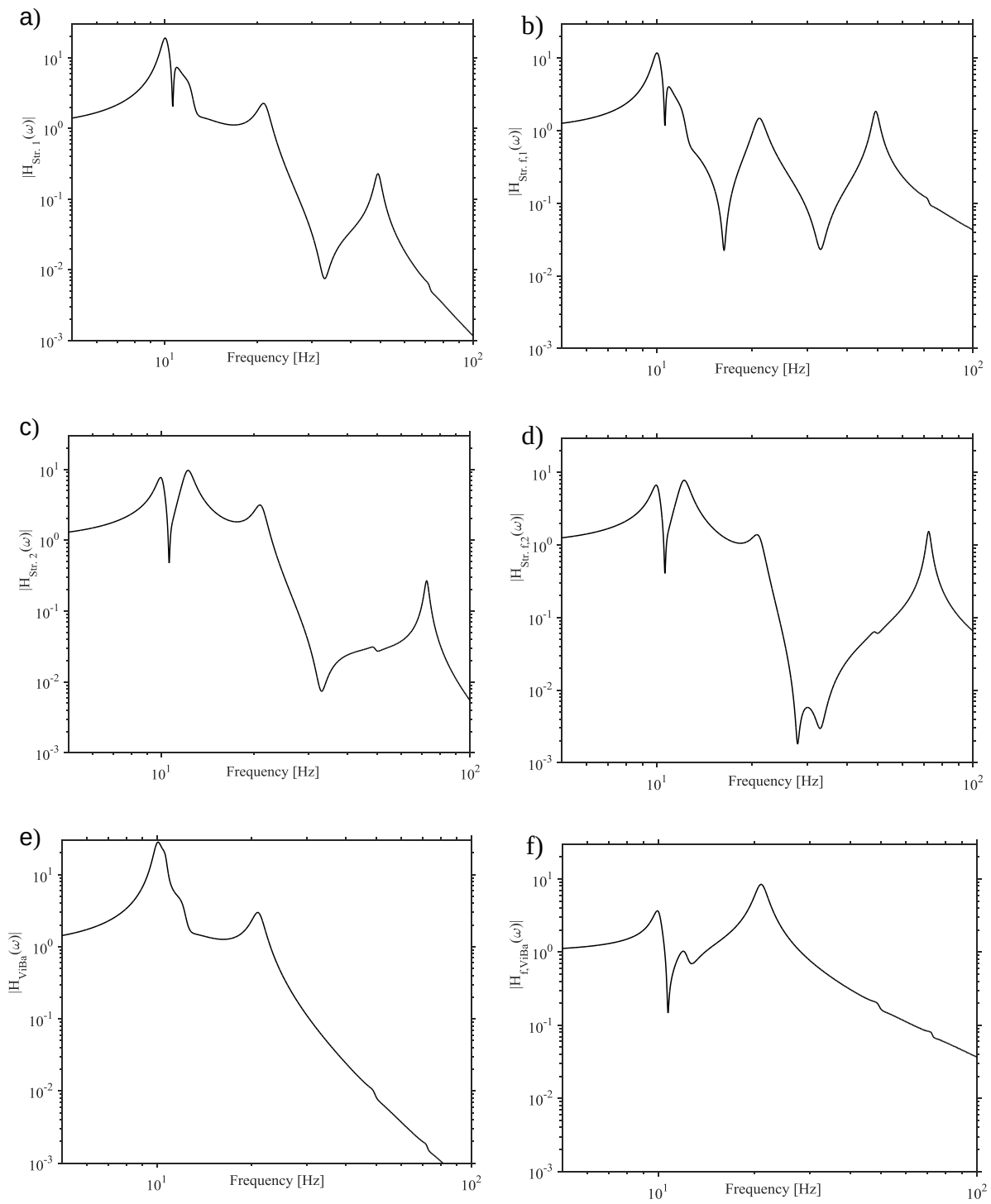

Fig. 7 Module of the transfer functions in logarithmic scale of the case with different structures coupled with ViBa for every degree of freedom: a) Structure 1, b) foundation 1, c) Structure 2 and d) foundation 2, e) VIBa and b) ViBa foundation.

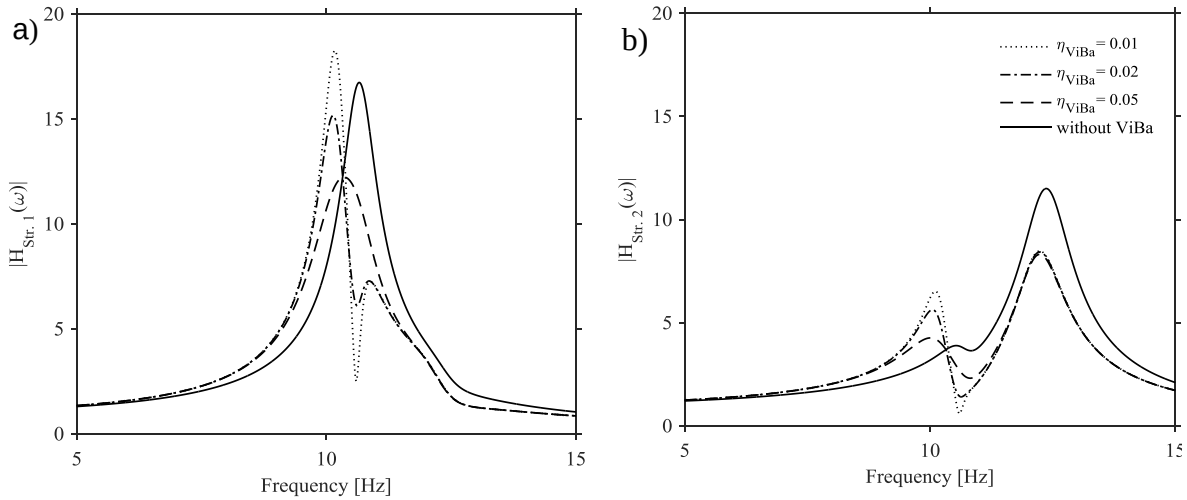

Fig. 8 Module of the transfer functions of a) Structure 1 and b) Structure 2 with different characteristics for several values of ViBa damping.

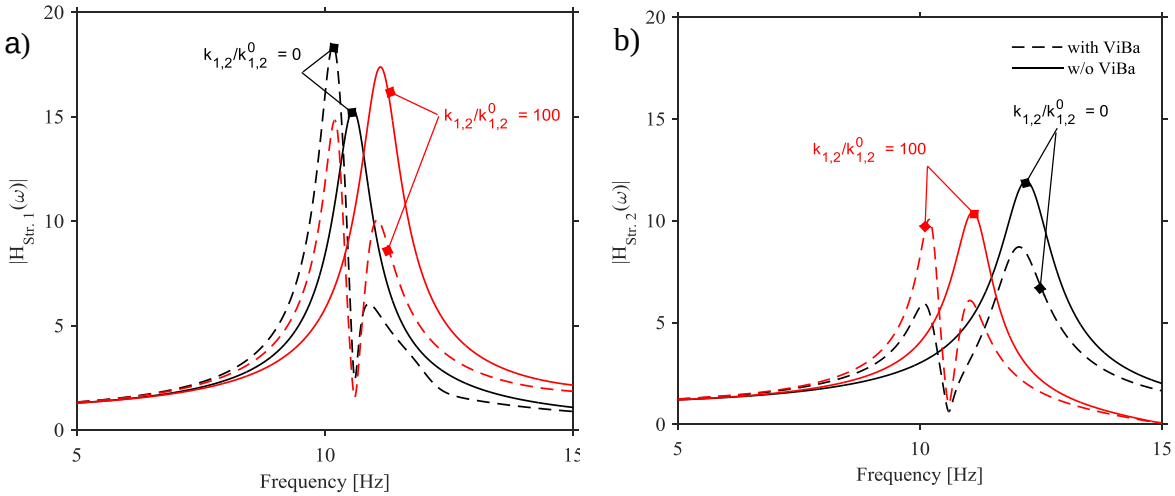

Fig. 9 Module of the transfer functions of a) Structure 1 and b) Structure 2 with different characteristics for several values of structure-soil-structure interaction.

Table 4 Characteristics of the structures and first natural frequencies

	Structure 1		**Structure 2**	
Case Study	**A**	**B-C**	**A**	**B-C**
Height [mm]	170		170	160
1st freq. [Hz]	10.68	10.71	10.68	11.23
1st freq. with trench [Hz]	10.7	10.8	10.77	11.3

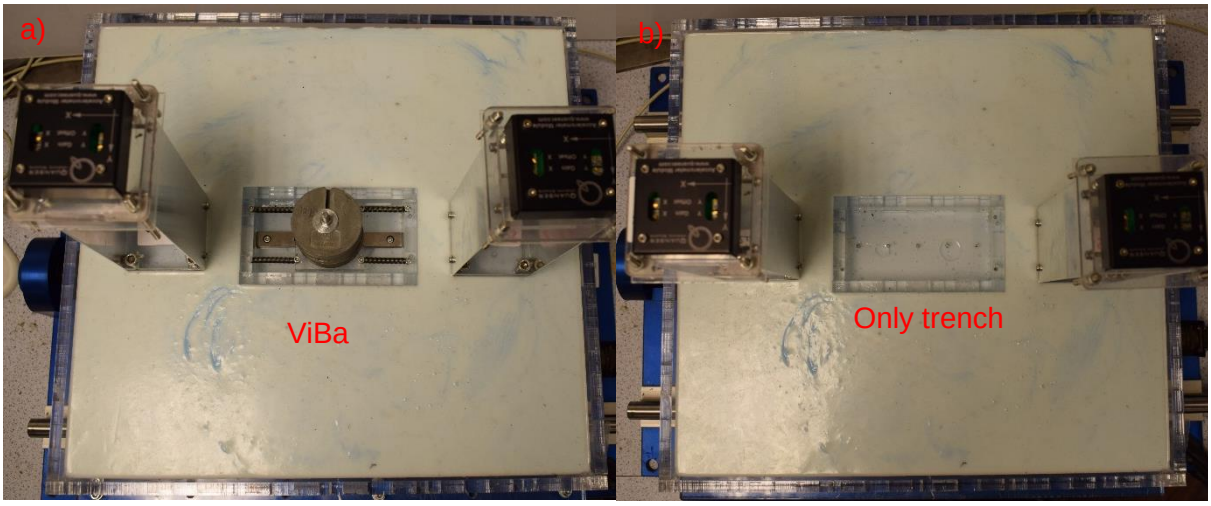

Fig. 10 Top view of the experimental shake table set-up a) with ViBa and b) without ViBa (with trench only).

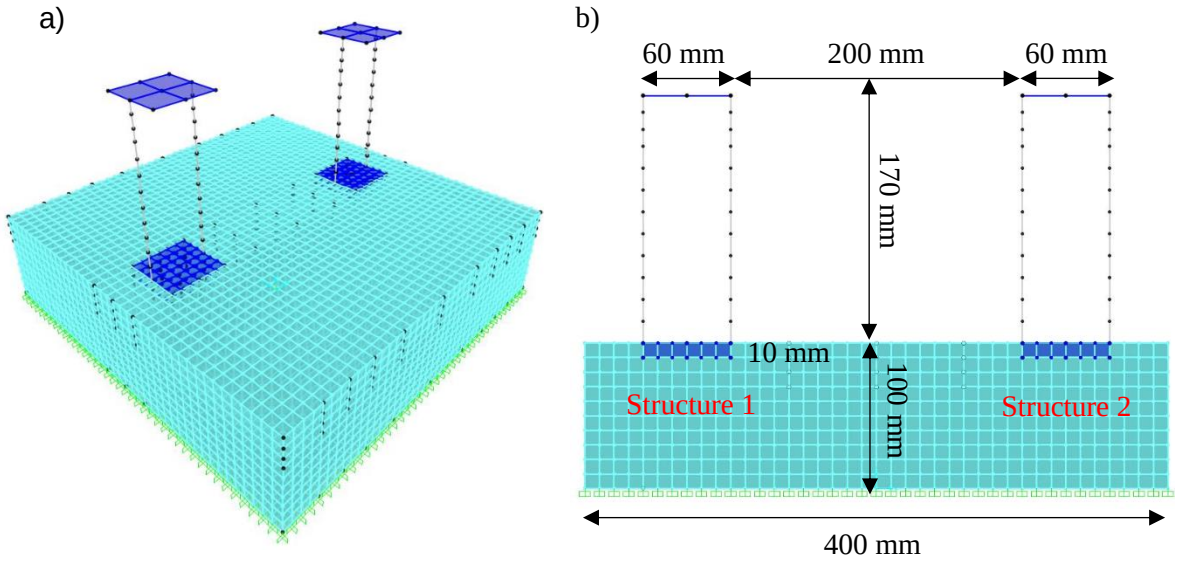

Fig. 11 Finite Element Model of the case study A (equal structures); a) 3D view and b) section view before construction of the ViBa.

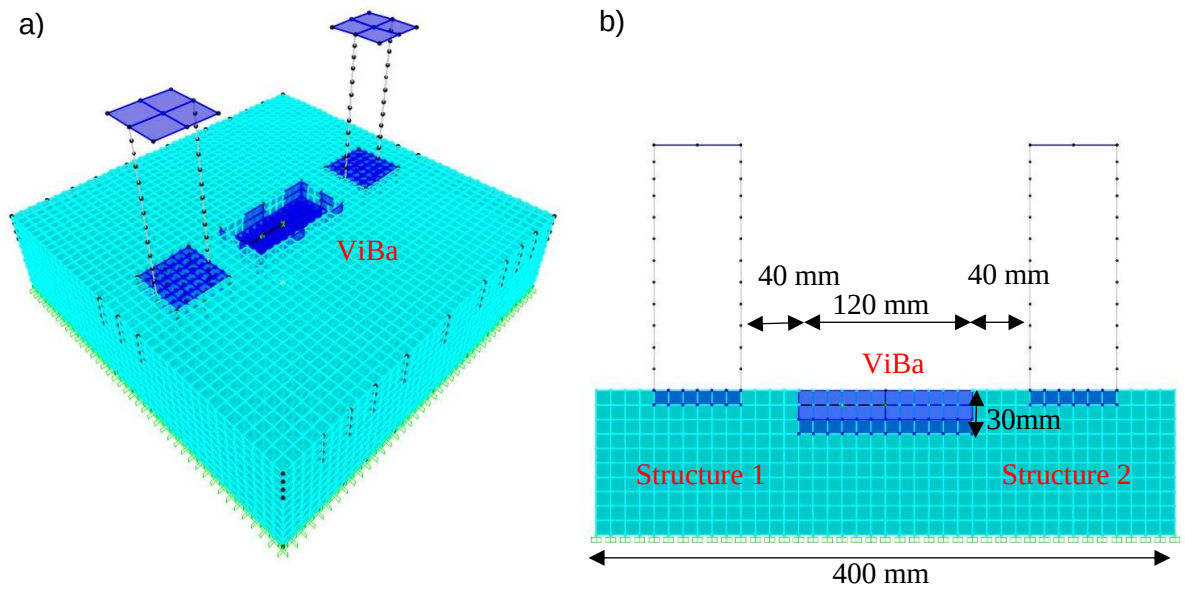

Fig. 12 Finite Element Model of the case study A (equal structures); a) 3D view; b) section view with ViBa.

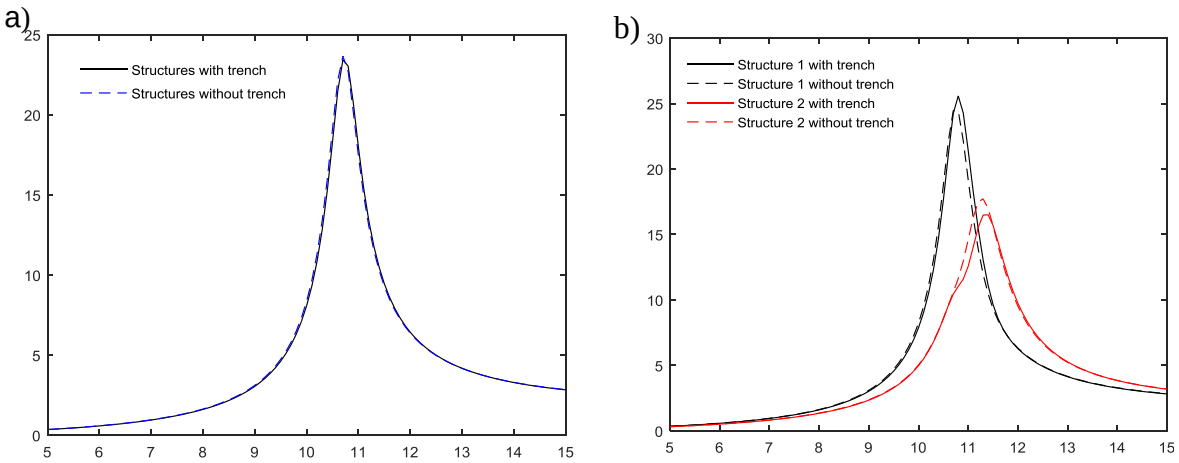

Fig. 13 Frequency response acceleration of Structure 1 and Structure 2 before and after realizing the trench for case a) A and b) B-C.

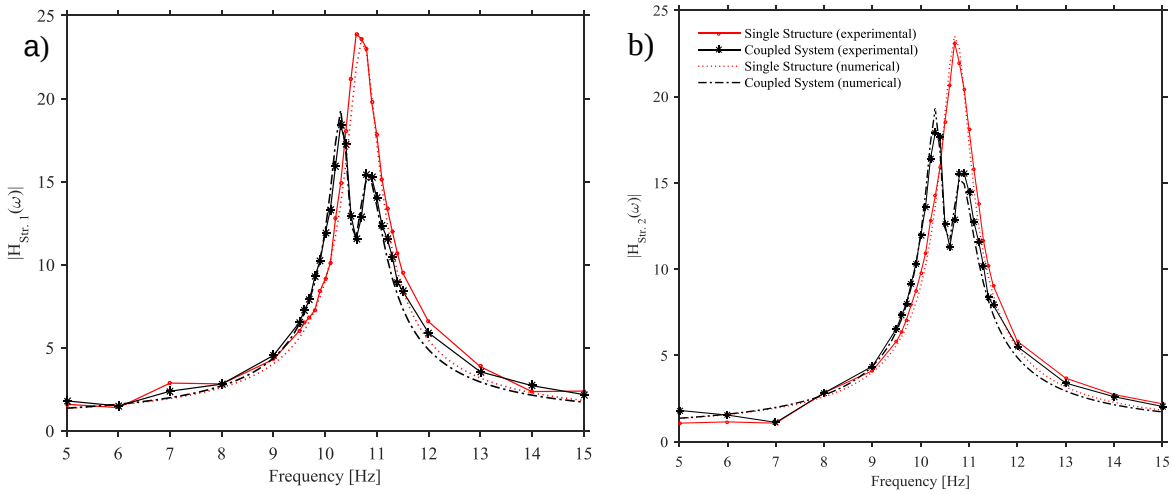

Fig. 14 Frequency response acceleration of a) Structure 1 and b) Structure 2 with and without the coupling with the ViBa for case study A.

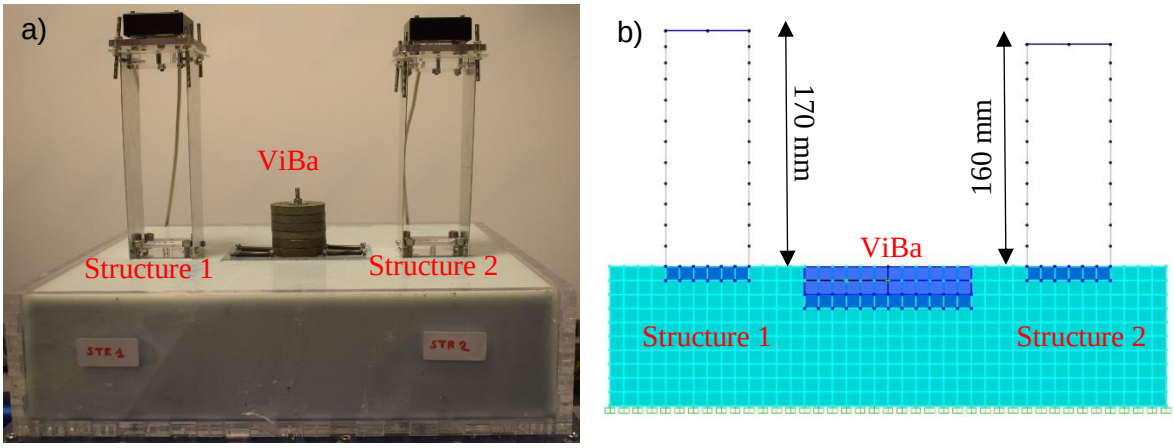

Fig. 15 Case Study B: a) Prototype and b) Finite Element Model of two different structures protected by the ViBa.

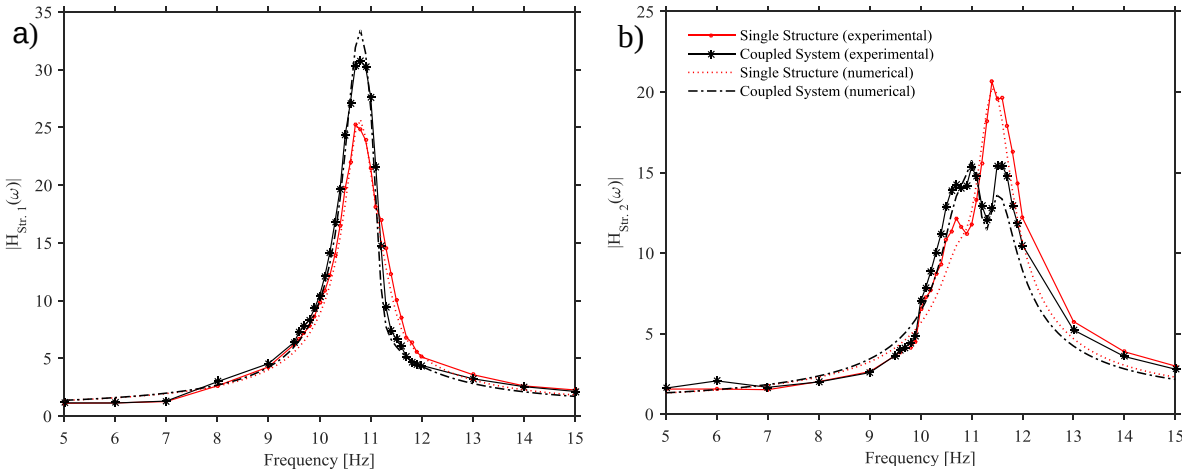

Fig. 16 Frequency response acceleration of a) Structure 1 and b) Structure 2 with and without the coupling with the ViBa for case study B.

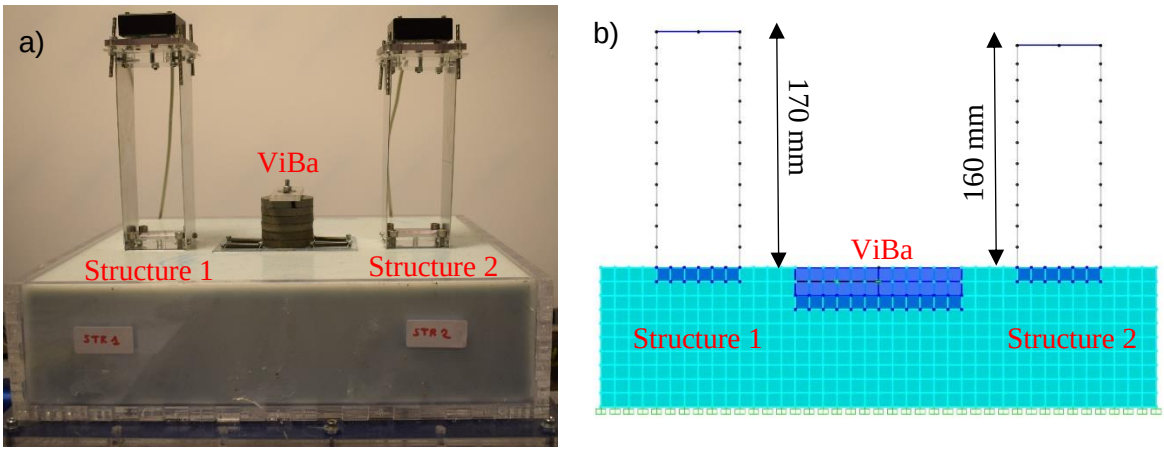

Fig. 17 Case study C: a) Prototype and b) Finite Element Model of two different structures protected by the ViBa.

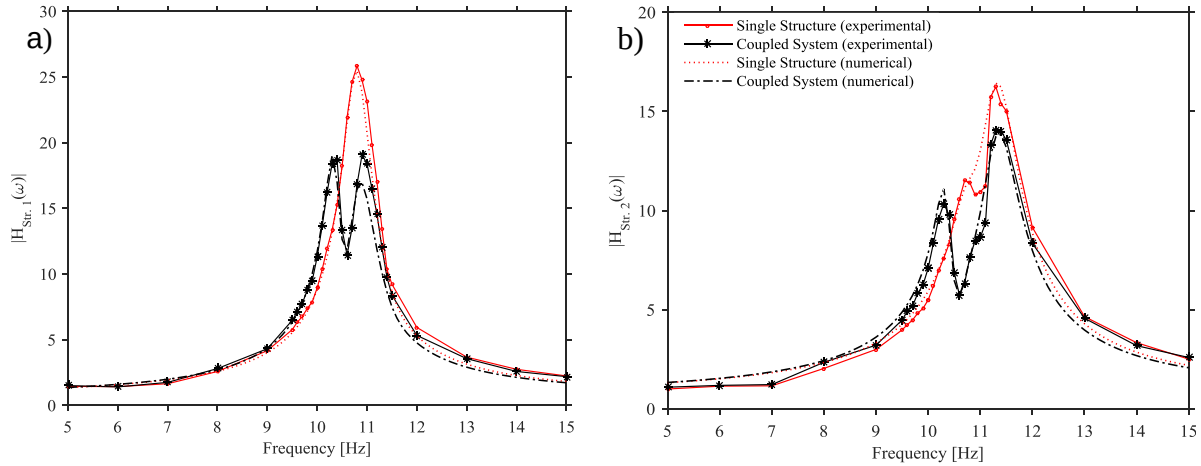

Fig. 18 Frequency response acceleration of a) Structure 1 and b) Structure 2 with and without the coupling with the ViBa for case study C.

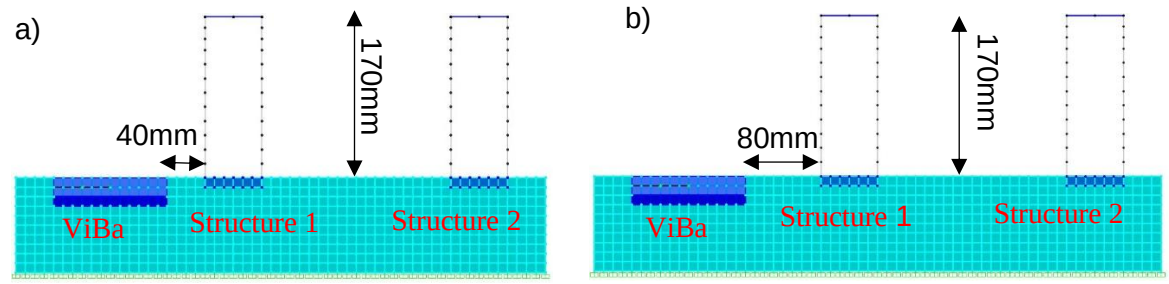

Fig. 19 Models for analysing the influence of the position of the Vibrating Barrier on the structural response of the cluster of buildings for a) Case 1 and b) Case 2.

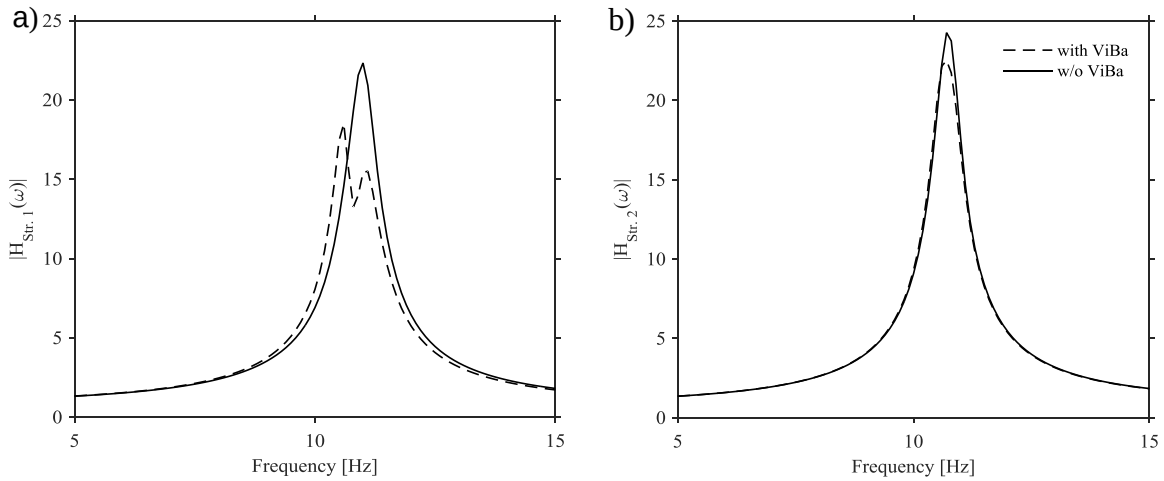

Fig. 20 Frequency response acceleration of a) Structure 1 and b) Structure 2 with and without the coupling with the ViBa for Case Study 1.

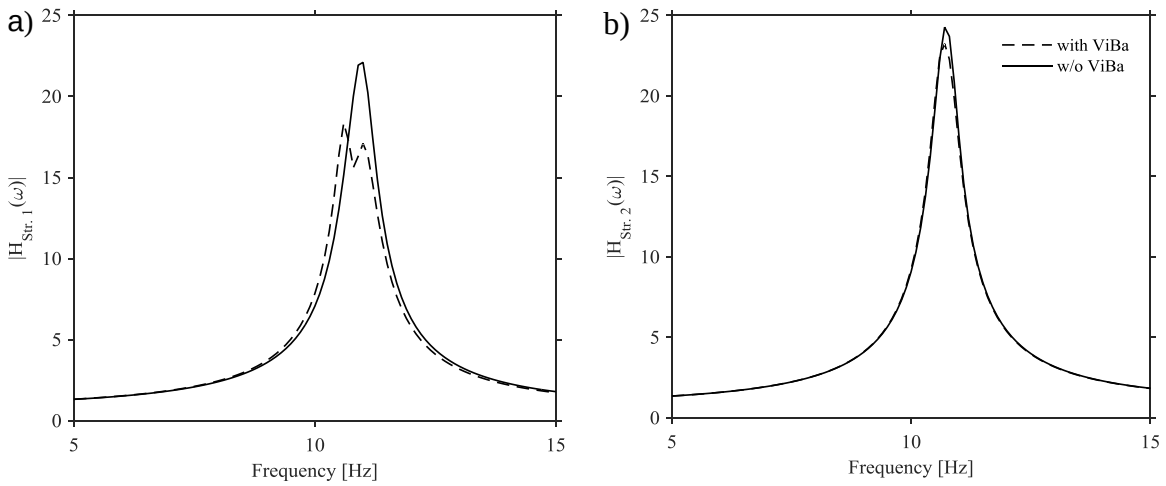

Fig. 21 Frequency response acceleration of a) Structure 1 and b) Structure 2 with and without the coupling with the ViBa for Case Study 2.